

The Effect of Mechanical Factors on Hydrogen Diffusion and Concentration around a Crack Tip

T. Ohmi¹, A. T. Yokobori Jr.¹, K. Takei²

¹ Graduate School of Engineering Tohoku University, Sendai, Japan

² Current affiliation; Kanto Auto Works, Ltd., Yokosuka, Japan

1. Introduction

Recently, the researches of hydrogen energy have been developed. However, the hydrogen penetrates into the metal and it causes hydrogen embrittlement. Concerning the investigation of hydrogen embrittlement, in spite of the fact that stiele studies have been conducted for many years, the mechanism of hydrogen embrittlement has not yet been clarified. For example, hydrogen embrittlement is typical for steels used for a petroleum-refining reactor. This will be due to the following reason. Hydrogen penetrates from a container wall surface when a petroleum-refining reactor operates under high temperature and pressurized hydrogen environmental conditions. Major part of the hydrogen remain in the wall for a long time during cooling process when the reactor is out of operation, which results in the delayed fracture [1,2]. Therefore, clarification of the hydrogen diffusion behavior in the metal is important for prevention of hydrogen embrittlement fracture.

To clarify the behavior of hydrogen embrittlement, the analysis of hydrogen diffusion and concentration is important and many researches have been conducted [3-13]. The basic equation of hydrogen diffusion and concentration is written by Eq. (1). Where $\nabla^2 \sigma_p = 0$ is valid in elastic region [3,4].

$$\frac{\partial C}{\partial t} = D \nabla \left(\nabla C + \alpha \frac{C}{RT} \nabla v \right) \quad (1)$$

$$v = -\sigma_p \Delta V$$

where C is hydrogen concentration, D is diffusion constant ($D = 12.7 \times 10^{-11} \text{ m}^2/\text{s}$ [3,4]), R is universal gas constant (8.314 Nm/molK), T is absolute temperature, t is time, ΔV is partial molar volume of hydrogen in the alloy considered ($2 \times 10^{-6} \text{ m}^3/\text{mol}$) [3,4], σ_p is hydrostatic stress.

In the plastic region, however $\nabla^2 \sigma_p$ is not equal to zero, the validity of the formulation of $W = -\sigma_p \Delta V$ is not clarified, since, volume dose not change in the plastic region. However, in the plastic region, as shown in Fig.1, since the region outside of slip band which is composed of dislocation is elastic, authors adopted Eq. (1) by substituting $\nabla^2 \sigma_p = 0$ into Eq. (1) in both elastic and plastic regions. Under constant stress condition, the analysis which is taken in to account for the term of $C \nabla^2 \sigma_p$ were also conducted, however, the mechanical effect of this term on hydrogen diffusion is not verified [9]. Furthermore by order estimation, the values of the second and third terms of the right hand side of Eq. (1) are one or two order lower than that of the first term [10-12]. Therefore, the method of

adding α to the second term, as the weight coefficient of the interaction factor written in the general formulation of transportation theory [14], has been proposed [10-12].

Concerning the third term, this concept will be also applicable. On the other hand, many analyses of hydrogen concentration have been conducted under constant stress condition, however, the analyses under stress rate or cycle loading condition are also important and part of authors has previously conducted the effect of stress waveform on hydrogen concentration around a crack tip under cycle loading [12].

In this paper, using Eq. (1) which includes the third term, the effect of stress rate, stress wave form, yield stress and temperature on hydrogen concentration around a crack tip were systematically analysed and the mechanical effect of $C \nabla^2 \sigma_p$ on hydrogen concentration was verified for the case when hydrogen penetrate into metal from outside.

2. Physical model and basic equation

The basic equation of hydrogen diffusion is essentially same as that of previous paper [10-12] and it is written by Eq. (1) with the addition of a stress induced diffusion [5,6]. In elastic region since $\nabla^2 \sigma_p$ is not zero in the plastic region, Eq. (1) reduces to

$$\frac{\partial C}{\partial t} = D \nabla C - \alpha \frac{D \Delta V}{RT} (\nabla C \cdot \nabla \sigma_p) . \quad (2)$$

In previous paper, Eq. (2) is also adopted for the analysis in plastic region. However, in this paper, since $\nabla^2 \sigma_p = 0$ is not valued, Eq. (3) is adopted in plastic region.

$$\frac{\partial C}{\partial t} = D \nabla C - \alpha \frac{D \Delta V}{RT} (\nabla C \cdot \nabla \sigma_p + C \nabla^2 \sigma_p) \quad (3)$$

Local elastic stress field around a crack tip is given by Eq. (4), [15]

$$\sigma_p = \frac{2}{3} (1 + \nu) \frac{K \cos(\theta / 2)}{\sqrt{2 \pi r}} + \frac{1}{3} \sigma_0 , \quad (4)$$

where ν is Poisson's ratio, K is stress intensity factor, σ_0 is gross stress.

Local plastic stress field around a crack tip is given by Eq. (5) [11,12] based on Hill's equation, [16]

$$\sigma_p = \frac{1}{3} (1 + \nu) \sigma_{ys} \left\{ 1 + 2 \ln \left(\frac{r}{\rho} \right) \right\} \cos \frac{\theta}{2} , \quad (5)$$

where ρ is crack tip radius, σ_{ys} is yield stress.

The basic equations for hydrogen diffusion and concentration around a crack tip are given by Eqs. (6) and (7) in the elastic and plastic region respectively.

Elastic region

$$\frac{\partial C}{\partial t} = D \left(\frac{\partial^2 C}{\partial r^2} + \frac{1}{r} \frac{\partial C}{\partial r} + \frac{1}{r^2} \frac{\partial^2 C}{\partial \theta^2} \right) + \frac{DK^*}{2RT} \left\{ \frac{\cos(\theta / 2)}{r^{3/2}} \frac{\partial C}{\partial r} + \frac{\sin(\theta / 2)}{r^{5/2}} \frac{\partial C}{\partial \theta} \right\} , \quad (6)$$

where $K^* = \frac{\sqrt{2}}{3} \frac{1}{\sqrt{\pi}} (1 + \nu) K \Delta V$.

Plastic region

$$\frac{\partial C}{\partial t} = D \left(\frac{\partial^2 C}{\partial r^2} + \frac{1}{r} \frac{\partial C}{\partial r} + \frac{1}{r^2} \frac{\partial^2 C}{\partial \theta^2} \right) + \frac{DU^*}{RT} \left[\frac{\sin(\theta/2)}{2r^2} \left\{ \frac{1}{2} + \ln\left(\frac{r}{\rho}\right) \right\} \frac{\partial C}{\partial \theta} - \frac{\cos(\theta/2)}{r} \frac{\partial C}{\partial r} + \frac{\cos(\theta/2)}{4r^2} C \left\{ \frac{1}{2} + \ln\left(\frac{r}{\rho}\right) \right\} \right] \quad (7)$$

where $U^* = \frac{2}{3}(1 + \nu)\sigma_{ys}\Delta V$.

Applied stress increases with increase in the time of stress application during loading process as shown in Eq. (8),

$$\sigma = \dot{\sigma}_R t \quad (8)$$

where $\dot{\sigma}_R$ is the applied loading rate. Correspondingly, the plastic region increases as is shown in Eq. (9),

$$r_Y = \frac{1}{2\pi} \left(\frac{K}{\sigma_Y} \right)^2 = \frac{a}{2} \left(\frac{\dot{\sigma} t}{\sigma_Y} \right)^2, \quad (9)$$

where r_Y is the distance of elastic plastic boundary from a crack tip.

The position of elastic plastic boundary was reset at the mesh point of finite difference element corresponding to the increase in r_Y . Yield stress, σ_Y is given by Eq. (10), [3,4]

$$\sigma_Y = P_C \sigma_{ys} = 1.125 \sigma_{ys}, \quad (10)$$

where P_C is plastic constraint coefficient, σ_{ys} is uniaxial tensile yield stress. Physical model and boundary condition were shown in Fig.1 and Fig.2. The crack length is 4.0×10^{-4} m and crack tip radius is 4.0×10^{-5} m. The analyses are using nondimensionalized variables:

$$r^+ = \frac{r}{a}, \quad C^+ = \frac{C}{C_0}, \quad t^+ = \frac{Dt}{a^2}.$$

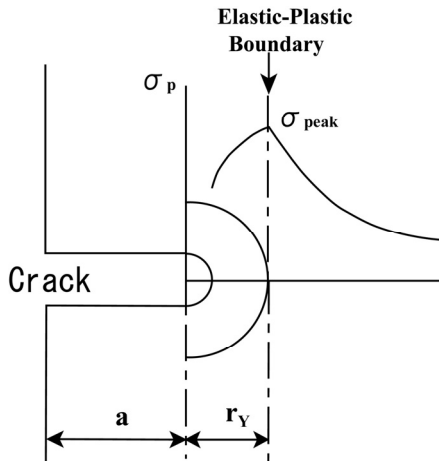


Fig.1 Physical model of elastic plastic local stress field around a crack tip.

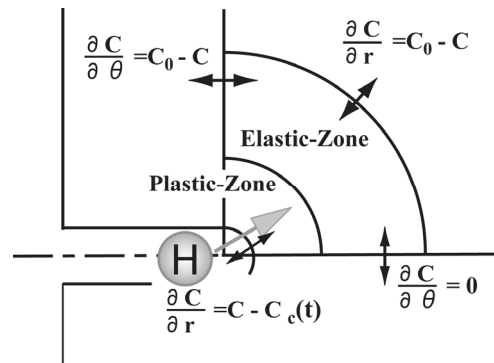


Fig.2 Physical model of hydrogen penetration and boundary condition.

3. Results of analysis under constant stress rate condition

3.1 The effect of stress rate

The effect of stress rate on hydrogen concentration is analyzed. Hydrogen originates from a crack tip surface and outer boundary to realize the hydrogen atmospheric condition. Eq. (11) is adopted as a function of hydrogen penetration, [11,12]

$$C_c(t) = (C_{c \max} - C_0) \{1 - \exp(-\eta t)\} + C_0, \quad (11)$$

where $C_{c \max}$ is maximum hydrogen emission concentration in the region of its penetration, C_0 is initial hydrogen concentration. η is a constant.

The result of order estimation was shown in Fig.3. As previously described, the value of first term is higher than that of second and third terms of the right hand side of Eq. (1). Referring to a past research [9-11], $\alpha = 100$ was used for the weight coefficient in this paper. By this method, we can analysis the dynamic effect of applied stress on the hydrogen concentration.

The behavior of hydrogen diffusion and concentration along the notch direction ($\theta = 0$ deg.) is shown in Fig.4 and Fig.5. It is shown that the hydrogen concentration at the elastic plastic boundary become higher under lower stress rate condition.

3.2 The effect of σ_{ys} under constant stress rate condition

To compare the effect of the yield stress on the hydrogen concentration systematically, the hydrogen concentration at the elastic plastic boundary is shown Fig.6. Hydrogen concentration increases with increase in the yield stress, and the effect of the stress rate on hydrogen concentration becomes critical. And the hydrogen concentrations become higher under lower stress rate

3.3 The effect of temperature under constant stress rate condition

To compare the effect of the temperature on the hydrogen concentration systematically, the hydrogen concentration at the elastic plastic boundary is shown Fig.7. Hydrogen concentration increases with decrease in temperature, and the effect of the stress rate becomes critical. And the hydrogen concentrations become higher under lower stress rate.

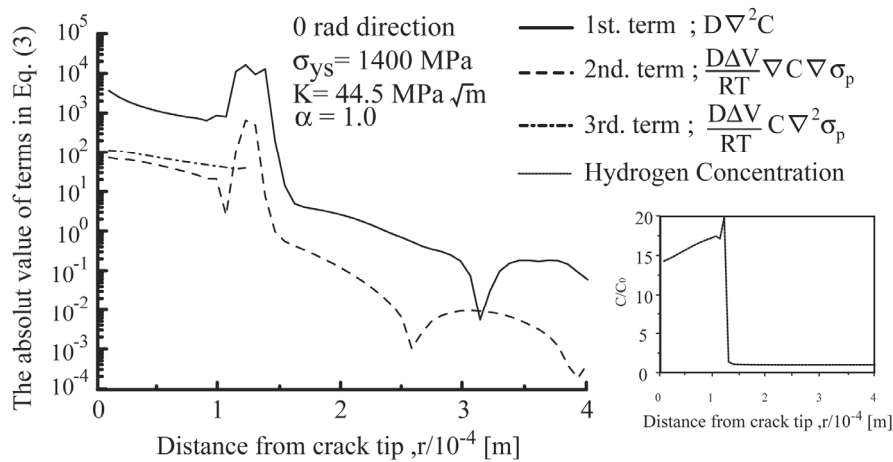


Fig.3 The value of each term in Eq.(3) at $\alpha=1.0$

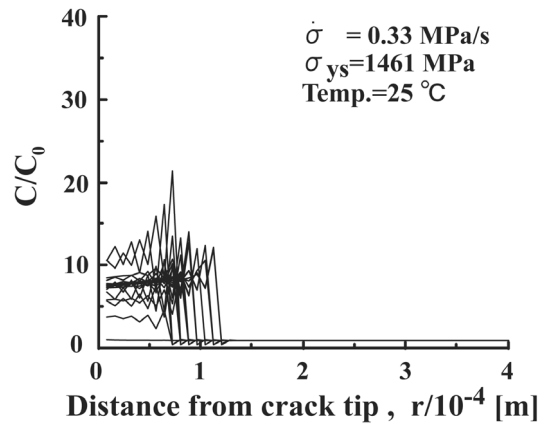


Fig.4 Numerical results on hydrogen concentration and distribution under high stress rate condition.

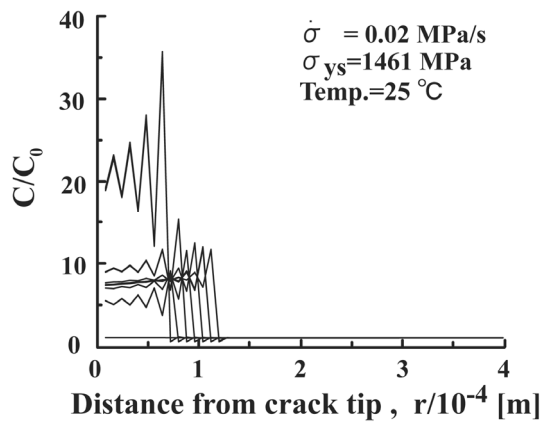


Fig.5 Numerical results on hydrogen concentration and distribution under low stress rate condition.

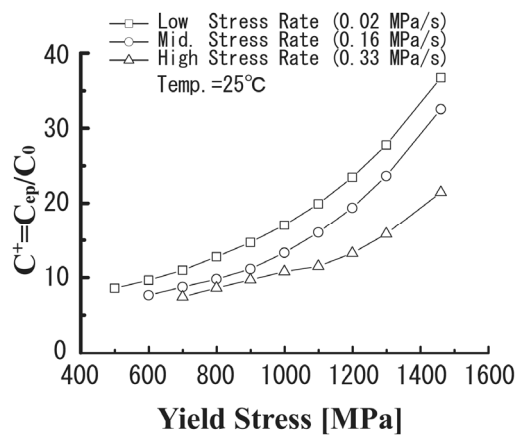


Fig.6 The effect of yield stress on hydrogen concentration at the elastic plastic boundary under constant stress rate.

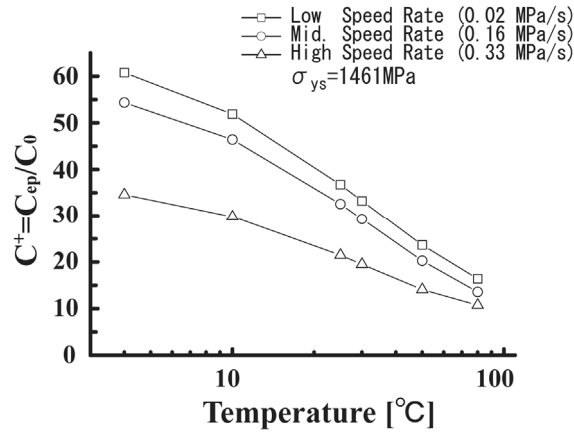


Fig.7 The effect of temperature on hydrogen concentration at the elastic plastic boundary under constant stress rate.

4. Results of analysis under cycle load condition

4.1 The effect of applied stress wave form

The effect of applied stress wave form on hydrogen concentration was analyzed. Due to the anodic dissolution reaction, hydrogen originates only from a crack tip surface. Eq. (12) is adopted as a function of hydrogen penetration under cycle loading condition (fatigue) [12],

$$\sigma_0(t) = \begin{cases} \dot{\sigma}_R t & (t < t_c) \\ \sigma_{max} - \dot{\sigma}_D (t - t_c) & (t \geq t_c) \end{cases}, \quad (12)$$

where σ_{max} is maximum applied stress, σ_R is stress rate of rising load, σ_D is stress rate of unloading. t_c is the time of maximum applied stress. The behavior of hydrogen diffusion and concentration along the notch direction ($\theta=0$ deg.) is shown in Fig.8 and Fig.9. It is shown that the hydrogen concentration at the elastic plastic boundary become higher under the Fast-Slow stress wave form condition.

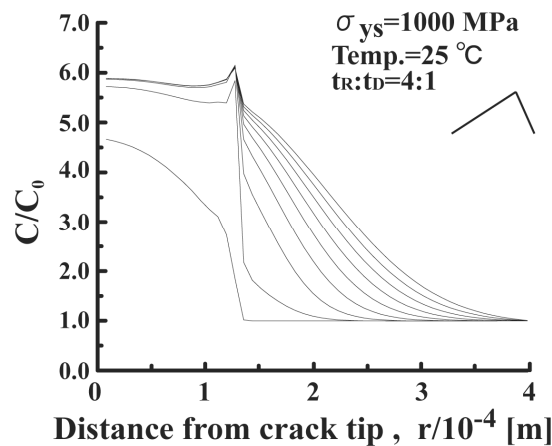


Fig.8 Numerical results on hydrogen concentration and distribution at the each load peak for 9 cycles under the Slow-Fast stress wave form

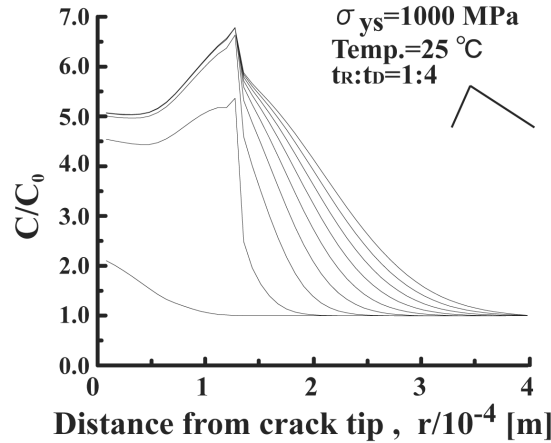


Fig.9 Numerical results on hydrogen concentration and distribution at the each load peak for 9 cycles under the Fast-Slow stress wave form

4.2 The effect of σ_{ys} under cycle load condition

To compare the effect of the yield stress on the hydrogen concentration systematically, the hydrogen concentration behavior at the elastic plastic boundary were shown Fig.10. The ratio of hydrogen concentration between notch tip and elastic plastic boundary was shown Fig.11. Hydrogen concentration increases with increase in the yield stress, and the effect of the stress wave form becomes critical. And the hydrogen concentrations become higher under the Fast-Slow stress wave form condition. These results mean the low unloading rate is a significant factor of hydrogen concentration.

These behaviors are qualitatively in good agreement with those obtained by previous paper which adopts Eq. (2) in plastic region. The term of $C \nabla^2 \sigma_p$ increases quantitatively the hydrogen concentration as shown in Fig.12.

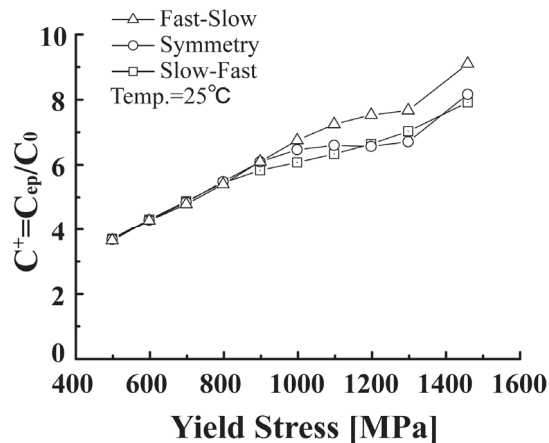


Fig.10 The effect of yield stress on hydrogen concentration at the elastic plastic boundary under cycle load condition.

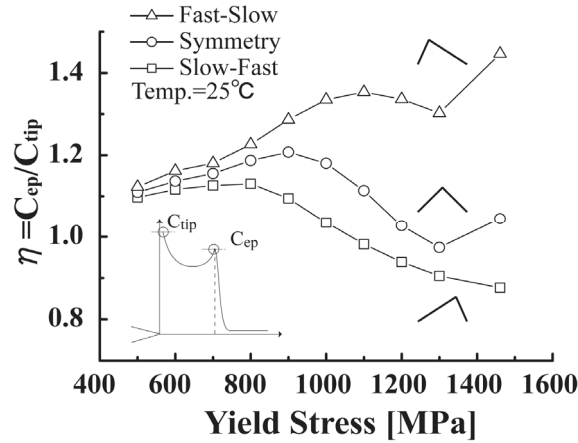


Fig.11 The effect of yield stress on the ratio of hydrogen concentration under cycle load condition.

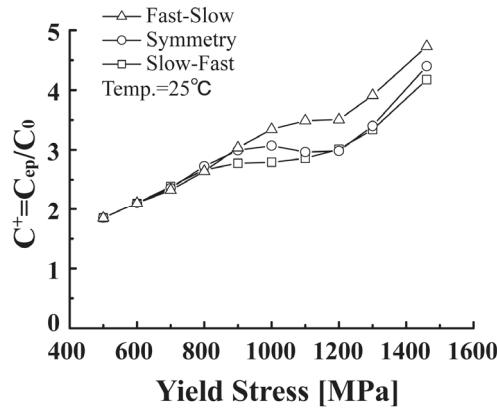


Fig.12 The effect of yield stress on hydrogen concentration at the elastic plastic boundary under cycle load condition by Eq. (2). ($\nabla^2 \sigma_p = 0$)

4.3 The effect of temperature under cycle load condition

To compare the effect of the temperature on the hydrogen concentration systematically, the hydrogen concentration at the elastic plastic boundary was shown Fig.13. And the ratio of hydrogen concentration between notch tip and elastic plastic boundary was shown Fig.14. Hydrogen concentration increases with decrease in temperature, and the effect of the stress wave form becomes critical. The hydrogen concentrations become higher under the Fast-Slow stress wave form condition. These results mean the low unloading rate is a significant factor of hydrogen concentration. These behaviors are qualitatively in good agreement with those obtained by previous paper which adopts Eq. (2) in plastic region. The term of $C \nabla^2 \sigma_p$ increases quantitatively the hydrogen concentration as shown in Fig.15.

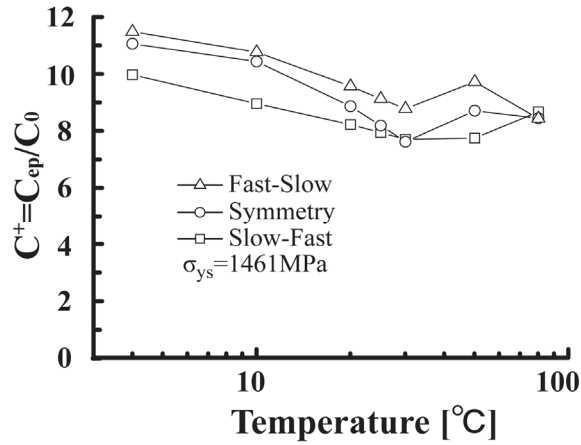


Fig.13 The effect of temperature on hydrogen concentration at the elastic plastic boundary under cycle load condition.

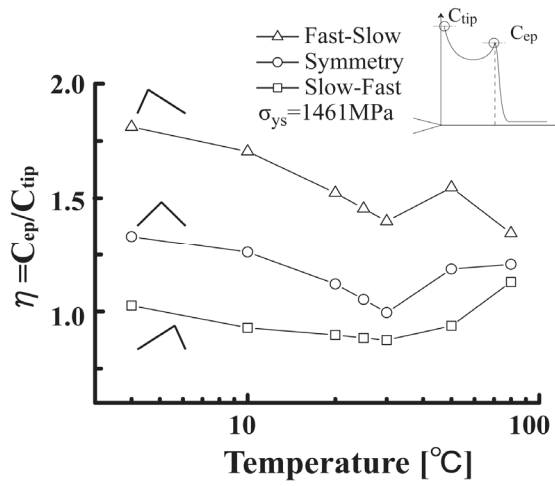


Fig.14 The effect of temperature on the ratio of hydrogen concentration under cycle load condition.

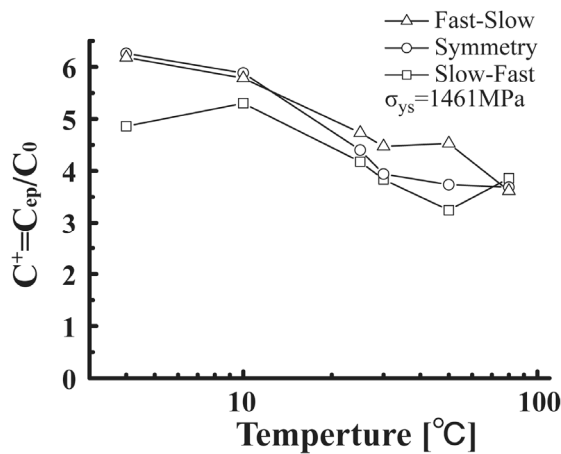


Fig.15 The effect of temperature on hydrogen concentration at the elastic plastic boundary under cycle load condition by Eq. (2). ($\nabla^2 \sigma_p = 0$)

5. Conclusion

Under the constant stress rate condition, the hydrogen concentration at the site of elastic plastic boundary becomes much more typical under the condition of low stress rate, high yield stress and low temperature. The stress rates dependence of hydrogen concentration becomes typical under high yield stress and low temperature.

Under the cyclic loading condition, the hydrogen concentration at the site of elastic plastic boundary becomes typical with increase in yield stress and decrease in temperature. Furthermore, concerning the effect of the stress wave form on the hydrogen concentration at the site of elastic plastic boundary, Fast-Slow stress wave form condition was found to promote hydrogen concentration at the site of elastic plastic boundary.

The third term of the basic equation quantitatively improves hydrogen concentration and the results of analysis are qualitatively well corresponding to the analysis which does not contain the term of $C \nabla^2 \sigma_p$.

6. References

- [1] K. Ohnishi, *Materia JAPAN*, 8 (1969) 576
- [2] Y. Wada, *Proc. of the 2003 Annual Meeting of the JSME/MMD*, (2003) 795
- [3] H.P. Leeuwen, *Engng. Fracture Mechanics*, 6 (1974) 141
- [4] H.P. Leeuwen, *Corrosion –NACE*, 31 (2) (1975) 42
- [5] R. Troiano, *J. Iron Steel Inst.*, 189 (5) (1958) 37,
- [6] R.A Oriani, *Hydrogen in metals*, In *Fundamental Aspects of Stress Corrosion Cracking* : R.W. Staehle, A.J. Forty, D. Van Rooyen (Eds.), NACE, Houston, 1969, 32
- [7] H.W. Liu, *Trans. ASME, J. Bas. Engng.* 92 (1970) 633.
- [8] M. Iino, *Engng. Fract. Mech.*, 10 (1978) 1.
- [9] P. Sofronis, R.M. McMeeking, *J. Mech. Phys. Solids*, 37 (3) (1989) 317-350
- [10] A. T. Yokobori Jr., T. Nemoto, K. Satoh, T. Yamada, *Engng. Fract. Mech.*, 5 (1996) 47
- [11] T. Yokobori Jr., Y. Chinda, T. Nemoto, K. Satoh, T. Yamada, *Corrosion Science* 44 (2002) 407-424
- [12] T. Yokobori Jr., T. Uesugi, M. Sendoh and M. Shibata, *Strength Fracture and Complexity An International Journal*, 1 (4) (2003) 187-204
- [13] A.H.M. Krom, R.W.J. Koers, A. Bakker, *J. Mech. Phys. Solids*, 47 (1999) 971-992
- [14] P. G. Shewmon, *Diffusion in solids*, Academic Press, New York, 1963, pp 122-125
- [15] M. Creager and P. C. Paris, *Int. J. Fracture Mech.*, 3 (1967) 247
- [16] R. Hill, *The Mathematical Theory of Plasticity*, Oxford University Press, Oxford, 1954, 242